Semi-analytical Monte Carlo optimisation method applied to the inverse Poisson problem

Sławomir Milewski[0000−0003−4967−9061]

Cracow University of Technology, Cracow, Poland
Faculty of Civil Engineering, Chair for Computational Engineering
s.milewski@L5.pk.edu.pl
https://www.cce.pk.edu.pl/ slawek/

Abstract. The research is focused on the numerical analysis of the inverse Poisson problem, namely the identification of the unknown (input) load source function, being the right-hand side function of the second order differential equation. It is assumed that the additional measurement data of the solution (output) function are available at few isolated locations inside the problem domain. The problem may be formulated as the non-linear optimisation problem with inequality constrains.
The proposed solution approach is based upon the well-known Monte Carlo concept with a random walk technique, approximating the solution of the direct Poisson problem at selected point(s), using series of random simulations. However, since it may deliver the linear explicit relation between the input and the output at measurement locations only, the objective function may be analytically differentiated with the respect to unknown load parameters. Consequently, they may be determined by the solution of the small system of algebraic equations. Therefore, drawbacks of traditional optimization algorithms, computationally demanding, time-consuming and sensitive to their parameters, may be removed. The potential power of the proposed approach is demonstrated on selected benchmark problems with various levels of complexity.

Keywords: inverse Poisson problem · optimisation problem · Monte Carlo method · meshless random walk

1 Introduction

Problems of computational mechanics and civil engineering may be classified as direct and inverse ones. In case of direct problems, the input data (geometry, material, load) are known and, therefore, the resulting initial-boundary problem remains well-posed and yields a unique output solution (displacement, temperature, flux, strain, stress), determined by means of rather numerical than analytical tools. However, in case selected input data are unknown, we deal with the inverse problem, either of topological optimisation or material/load identification nature. Additional information is required, for instance optimisation criteria (e.g., minimal mass or maximal capacity) or measurement data of output functions at selected points of the problem domain and its boundary. The

ICCS Camera Ready Version 2021
To cite this paper please use the final published version:
DOI: 10.1007/978-3-030-77970-2_19

optimal number of measurements as well as their appropriate locations are substantial since ill-posed inverse problems, suffering from information shortage, are usually ill-conditioned (in Hadamard sense) and, therefore, extremely sensitive to small data modifications.

Load identification problems are considered in this research, being the important stage of the recovery process of the full current static/dynamic/thermal state of existing engineering constructions. This process is usually based upon non-destructive, contact (e.g., sensors attached to the construction) or non-contact (e.g., vision techniques) measurements, done at few selected locations (nodes, bars, surfaces). In this manner, the determination of the current state of the structure allows for the estimation of time of its safe operation and exploitation, which is a part of a wide range of SHM (Structural Health Monitoring) issues.

The attention is laid upon the Poisson differential equation, modelling a variety of processes occurring in nature, for instance the gravitational field potential in the presence of sources, selected linear elasticity problems (torsional deflection of a prismatic bar, plane stress/plane strain/axial symmetry), stationary heat flow, distribution of electric potential, or filtration through porous systems. In case of the inverse Poisson problem, the source load (input) function, being the right-hand side function of the Poisson equation, is considered as the additional unknown, along with the primary output function. The source function may be interpreted, for instance, as the intensity of an external live load, subjected to the construction, or as the intensity of a heat generation inside the domain. Since it cannot be directly measured, its comprehensive determination (values, support, localization, gradient) is crucial for the entire solution procedure.

The solution approach to inverse source problems strongly depends on the type of additional data. The simplest and rather not realistic cases, though allowing for the avoidance of the ill-conditioning, assume the existence of a continuous input/output solution, partially given on the boundary and/or inside the domain. Therefore, the original heterogeneous problem (with non-zero unknown source function) may be transformed into the auxiliary homogeneous problem, being solved using traditional computational tools, like Finite Element Method (FEM) [1], Boundary Element Method (BEM) [2], Finite Difference Method (FDM) or meshless methods [3, 4], and then retransformed. The iterative algorithm with the source function, partially known on the boundary, is presented in [5]. Consideration of noisy data requires additional restoration algorithms, usually of probabilistic type, preceding an reverse transform [6, 7]. On the other hand, more experimentally oriented approaches take real measurement data into account. Measurements, with assigned uncertainties, have fixed locations or may be arbitrarily scattered in the problem domain. Consequently, the non-linear optimisation problem is formulated and solved [8, 9], incorporating aforementioned deterministic (FEM, FDM, meshless methods [10, 11]) as well as stochastic solution approaches (genetic algorithms, neural networks [12, 13]). Ill-conditioning of the original inverse problem is reduced by appropriate regularization techniques [10, 14].

ICCS Camera Ready Version 2021
To cite this paper please use the final published version:
DOI: 10.1007/978-3-030-77970-2_19

Although a variety of optimisation methods exists, most of them exhibit serious drawbacks, for instance time–consuming searching algorithms (non-gradient methods), computationally demanding multiple solutions of auxiliary differential problems for fixed source parameters, numerical evaluation of the objective function's gradient and/or Hessian, sensitiveness to initial guess solutions (for iterative procedures) as well as requirement for admissible solution intervals. The proposed Monte Carlo optimization method allows for the reduction of those disadvantages. It is based upon the old concept of the Monte Carlo (MC) method with a random walk technique for an approximate solution of the Laplace problem at the selected point of the rectangular grid of points [15]. Series of simulations (random walks) are performed, starting from the considered point and terminating at the boundary, where the solution is known. Sum of all boundary indication numbers, related to the total number of trials and scaled by boundary solution values, is an unbiased estimator of the Laplace problem at this point. Moreover, it is convergent to the corresponding finite difference (FD) solution of the same problem, providing the number of trials is large enough [16, 17].

Its novel application to inverse source problems assumes the determination of indication numbers, separately for all measurement points, coinciding with approximation nodes, regardless of their distribution. Afterwards, resultant explicit relations between the input (source function parameters) and output (solution values at measurement points) may be substituted into the objective function, minimising the measurement error. This move allows for its analytical differentiation towards fulfilment of the necessary condition of the existence of its extreme. Eventually, one obtains small symmetric system of algebraic equations. Once the source function is recovered, the problem becomes a direct one, and the unknown output function along with its derivatives may be determined using standard computational tools. The entire solution procedure is a two-step one and it does not require any a-priori knowledge concerning the unknown solution and source function. The solution of the inverse problem is obtained in an explicit form, using semi-analytical transformations, based upon combined, stochastic (MC)–deterministic (FD) model.

The paper is organized in the following manner. Section 2 presents the formulation of the analysed inverse problem. Section 3 introduces the source function recovery, using either its global approximation or independent approximation mesh. Section 4 presents results of several benchmark problems. The paper is briefly concluded and directions of future work are indicated.

2 Formulation of the inverse Poisson problem

The following 2D Poisson equation is considered

$$\boldsymbol{\nabla}^2 F = f(\mathbf{x}) \quad \text{in} \quad \Omega \tag{1}$$

with essential boundary conditions

$$F = \bar{F}(\mathbf{x}) \quad \text{on} \quad \partial\Omega \tag{2}$$

ICCS Camera Ready Version 2021
To cite this paper please use the final published version:
DOI: 10.1007/978-3-030-77970-2_19

where $\boldsymbol{\nabla}^2 = \boldsymbol{\Delta} = \dfrac{\partial^2}{\partial x_1^2} + \dfrac{\partial^2}{\partial x_2^2}$ is the Laplace operator, $\Omega = \{\mathbf{x} = \left[x_1 \; x_2 \right]\} \in \Re^2$ is the problem domain, $\partial\Omega$ – its boundary, $F : \mathbf{x} \in \Omega \to \Re$ is the unknown C^2 scalar output function, with given values $\bar{F}(\mathbf{x})$ at every boundary point $\mathbf{x} \in \partial\Omega$.

It is assumed that the right–hand side input function $f = f(\mathbf{x})$ is unknown and has to be determined on the basis of additional data

$$\hat{F}_k \pm \Delta F, \quad k = 1, 2, ..., m \tag{3}$$

being measurements $\hat{F}_k$ of the output function F with given tolerance ΔF at m measurement points $\hat{\mathbf{x}}_k = \left[\hat{x}_1^{(k)} \; \hat{x}_2^{(k)} \right]$. Furthermore, let us assume that the unknown function f is represented by the finite set of its n_f parameters (degrees of freedom), denoted as $\boldsymbol{\alpha} = \left[\alpha_1 \; \alpha_2 \; ... \; \alpha_{n_f} \right]$. Therefore, coefficients of $\boldsymbol{\alpha}$ constitute the set of primary unknowns to the considered inverse problem and $F = F(\mathbf{x}, \boldsymbol{\alpha})$, $f = f(\mathbf{x}, \boldsymbol{\alpha})$. The relevant non–linear optimisation problem may be formulated, namely find such optimal parameters

$$\boldsymbol{\alpha}_{\text{opt}} = \text{argmin}_{(\boldsymbol{\alpha})} J(\boldsymbol{\alpha}) \tag{4}$$

that minimise the following objective function

$$J(\boldsymbol{\alpha}) = \sqrt{\frac{1}{m} \sum_{k=1}^{m} \left(\frac{F(\hat{\mathbf{x}}_k, \boldsymbol{\alpha}) - \hat{F}_k}{\Delta F} \right)^2} \tag{5}$$

with inequality constraints

$$\left| F(\hat{\mathbf{x}}_k, \boldsymbol{\alpha}) - \hat{F}_k \right| < \Delta F, \quad k = 1, 2, ..., m \tag{6}$$

where $F(\hat{\mathbf{x}}_k, \boldsymbol{\alpha})$ are values of F at measurement points. The necessary condition of the existence of the extreme of (5) is

$$\boldsymbol{\nabla}_{\boldsymbol{\alpha}} J(\boldsymbol{\alpha}) = \mathbf{0} \tag{7}$$

which leads to the algebraic system of n_f equations with n_f unknowns. After substitution of (5) to (7), one obtains the following expression

$$\boldsymbol{\nabla}_{\boldsymbol{\alpha}} J(\boldsymbol{\alpha}) = \sum_{k=1}^{m} \left(F(\hat{\mathbf{x}}_k, \boldsymbol{\alpha}) - \hat{F}_k \right) \boldsymbol{\nabla}_{\boldsymbol{\alpha}} F(\hat{\mathbf{x}}_k, \boldsymbol{\alpha}) \tag{8}$$

in which $\boldsymbol{\nabla}_{\boldsymbol{\alpha}} F$ is the $[n_f \times 1]$ gradient vector

$$\boldsymbol{\nabla}_{\boldsymbol{\alpha}} F(\mathbf{x}, \boldsymbol{\alpha}) = \left\{ \frac{\partial F}{\partial \alpha_l}, \quad l = 1, 2, ..., n_f \right\} \tag{9}$$

The sufficient condition of the existence of the minimum of (5) is the positive-definitiveness of the Hesse matrix (Hessian) of (5), defined as $\mathbf{H}(\boldsymbol{\alpha}) = \boldsymbol{\nabla}_{\boldsymbol{\alpha}}^2 J(\boldsymbol{\alpha})$, which corresponds to the convex objective function.

ICCS Camera Ready Version 2021
To cite this paper please use the final published version:
DOI: 10.1007/978-3-030-77970-2_19

3 Recovery of the source function

Let us assume that the square grid Ω_h with boundary $\partial\Omega_h$, represented by one mesh modulus h and consisting of n_F nodes $\mathbf{x}_F \in \Omega_h$, has been generated. Therefore, each node $\mathbf{x}_F$ may be expressed using two indices (i,j), namely $\mathbf{x}_{i,j} = \left[x_1^{(i,j)}\ x_2^{(i,j)}\right]$ (Fig 1a). Applying the finite difference solution approach to (1), we replace the differential operators with difference ones, using appropriate configurations of nodes (stars) as well as we generate difference equations at internal nodes using collocation technique, namely

$$\frac{F_{i-1,j} + F_{i,j+1} + F_{i+1,j} + F_{i,j-1} - 4F_{i,j}}{h^2} = f_{i,j} \tag{10}$$

By terms rearrangement, we obtain the relation between the central value of a star and the remaining ones

$$F_{i,j} = \frac{1}{4}F_{i-1,j} + \frac{1}{4}F_{i,j+1} + \frac{1}{4}F_{i+1,j} + \frac{1}{4}F_{i,j-1} - \frac{h^2}{4}f_{i,j} \tag{11}$$

which factors may be considered as probabilities of selection of a next move within each random walk component, equal for each sense of directions (top, right, bottom, left). The final Monte Carlo formula

$$F_{i,j} \approx \frac{1}{N}\left(\sum_{(r,s)\in\partial\Omega_h} \bar{F}_{r,s}\bar{N}_{(i,j),(r,s)} - \frac{h^2}{4}\sum_{(r,s)\in\Omega_h} f_{r,s}N_{(i,j),(r,s)}\right), \quad (i,j)\in\Omega_h \tag{12}$$

is the stochastic approximation of all a–priori known problem parameters. Here, N denotes the total number of all random walks, terminating at boundary nodes $\mathbf{x}_{r,s} = \left[x_1^{(r,s)}\ x_2^{(r,s)}\right] \in \partial\Omega_h$ with known solution values $\bar{F}_{r,s}$. Moreover, $\bar{N}_{(i,j),(r,s)}$ and $N_{(i,j),(r,s)}$ denote nodal indications, being the number of hits of each boundary node (r,s), and the number of visits of each internal node (r,s), respectively, for a random walk starting from the internal node (i,j). Error bounds of (12) may be estimated using the a–priori formula

$$e = \left|\frac{F_{i,j} - F_{i,j}^{fdm}}{F_{i,j}^{fdm}}\right| < \frac{1}{\sqrt{N}} \tag{13}$$

where $F_{i,j}^{fdm}$ is the corresponding finite difference solution of (1) at the internal node (i,j).

3.1 Simplest constant approximation

In case we expect the unknown source function to be a smooth one, namely values of its gradient are small, we may use the simplest constant approximation of f, in order to have the general impression concerning its basic features. Therefore,

ICCS Camera Ready Version 2021
To cite this paper please use the final published version:
DOI: 10.1007/978-3-030-77970-2_19

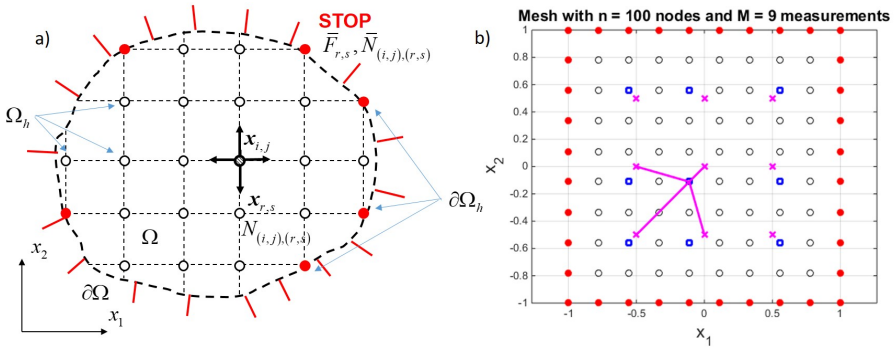

Fig. 1. Scheme of random walks for a regular grid of point (a) as well as exemplary regular distributions of approximation nodes $\mathbf{x}_F$ of F (red and white circles), measurements $\hat{\mathbf{x}}$ (blue squares) and approximation nodes $\mathbf{x}_f$ of f (magenta crosses) with a meshless star for a local approximation of f at $\mathbf{x}_F$ (b)

we assume that the function f is ascribed by one unknown constant parameter $\alpha_1 = f = const$. In that case, the Monte Carlo relation (12) becomes

$$F_{i,j}(f) = \frac{1}{N}\left(\sum_{(r,s)\in\partial\Omega_h} \bar{F}_{r,s}\bar{N}_{(i,j),(r,s)} - \frac{h^2 f}{4}\sum_{(r,s)\in\Omega_h} N_{(i,j),(r,s)}\right) \tag{14}$$

Condition (7) of existence of extreme solution $\dfrac{dJ}{df} = 0$ leads to the following equation

$$\sum_{i,j}^{m}\left(F_{i,j}(f) - \hat{F}_{i,j}\right)\sum_{(r,s)\in\Omega_h} N_{(i,j),(r,s)} = 0 \tag{15}$$

which solution may be explicitly determined

$$f_{\text{opt}} = \frac{4\sum_{i,j}^{m}\left(\bar{S}_{i,j}S_{i,j} - N\hat{F}_{i,j}S_{i,j}\right)}{h^2\sum_{i,j}^{m} S_{i,j}^2}, \quad \begin{cases} \bar{S}_{i,j} = \sum\limits_{(r,s)\in\partial\Omega_h} \bar{F}_{r,s}\bar{N}_{(i,j),(r,s)} \\ S_{i,j} = \sum\limits_{(r,s)\in\Omega_h} N_{(i,j),(r,s)} \end{cases} \tag{16}$$

in a stochastic, semi-analytical manner. Since f_{opt} corresponds to the analytical solution of (7), the inequality constraints (6) are a–priori satisfied.

3.2 Global approximation of an arbitrary order

More general approximation of the unknown source function on the global level may incorporate the vector of n_f degrees of freedom $\boldsymbol{\alpha}$ as well as the vector of

ICCS Camera Ready Version 2021
To cite this paper please use the final published version:
DOI: 10.1007/978-3-030-77970-2_19

n_f global basis functions $\mathbf{\Phi} = \{\Phi_l,\ l = 1, 2, ..., n_f\}$, namely

$$f(\mathbf{x}, \boldsymbol{\alpha}) = \sum_{l=1}^{n_f} \alpha_l\ \Phi_l(\mathbf{x}) = \boldsymbol{\alpha}\ \mathbf{\Phi}(\mathbf{x}) \tag{17}$$

In most approaches, degrees of freedom $\boldsymbol{\alpha}$ are values of f (physical degrees of freedom), providing basis functions are dimensionless (e.g., standard shape functions). However, since the initial values of $\boldsymbol{\alpha}$ are not required here, $\boldsymbol{\alpha}$ may be arbitrary mathematical degrees of freedom whereas basis functions may be simple monomials. On the basis of the Monte Carlo relation

$$F_{i,j}(\boldsymbol{\alpha}) = \frac{1}{N}\left(\sum_{(r,s)\in\partial\Omega_h} \bar{F}_{r,s}\bar{N}_{(i,j),(r,s)} - \frac{h^2}{4}\sum_{(r,s)\in\Omega_h} \boldsymbol{\alpha}\ \mathbf{\Phi}(\hat{\mathbf{x}}_{r,s})\, N_{(i,j),(r,s)}\right) \tag{18}$$

as well as the necessary conditions

$$\frac{\partial J}{\partial \alpha_l} = \sum_{i,j}^{m}\left(F_{i,j}(\boldsymbol{\alpha}) - \hat{F}_{i,j}\right)\sum_{(r,s)\in\Omega_h} \Phi_l(\hat{\mathbf{x}}_{r,s})\, N_{(i,j),(r,s)} = 0, \quad l = 1, 2, ..., n_f \tag{19}$$

we obtain the symmetric and positive–definite system of linear equations which solution may be expressed in the following matrix notation

$$\mathbf{A}\boldsymbol{\alpha}_{\text{opt}} = \mathbf{B}, \quad \boldsymbol{\alpha}_{\text{opt}} = \mathbf{A}^{-1}\mathbf{B} \tag{20}$$

where

$$A_{k,l} = \sum_{i,j}^{m} S_{i,j}^{(k)} S_{i,j}^{(l)}, \quad B_k = \frac{4}{h^2}\sum_{i,j}^{m}\left(\bar{S}_{i,j} - N\hat{F}_{i,j}\right) S_{i,j}^{(k)}, \quad k, l = 1, 2, ..., p$$

$$\bar{S}_{i,j} = \sum_{(r,s)\in\partial\Omega_h} \bar{F}_{r,s}\bar{N}_{(i,j),(r,s)}, \quad S_{i,j}^{\{(k),(l)\}} = \sum_{(r,s)\in\Omega_h} \Phi_{\{k,l\}}(\hat{\mathbf{x}}_{r,s})\, N_{(i,j),(r,s)} \tag{21}$$

For instance, the linear approximation of f ($n_f = 3$) may be assumed as

$$f(\mathbf{x}, \boldsymbol{\alpha}) = \alpha_1\Phi_1(\mathbf{x}) + \alpha_2\Phi_2(\mathbf{x}) + \alpha_3\Phi_3(\mathbf{x}) = \alpha_1 + \alpha_2 x_1 + \alpha_3 x_2 \tag{22}$$

whereas the optimal set of mathematical degrees of freedom $\boldsymbol{\alpha} = \begin{bmatrix}\alpha_1 & \alpha_2 & \alpha_3\end{bmatrix}$ may be obtained from (20), namely

$$\begin{bmatrix} \sum_{i,j}^{m}\left(S_{i,j}^{(1)}\right)^2 & \sum_{i,j}^{m} S_{i,j}^{(2)}S_{i,j}^{(1)} & \sum_{i,j}^{m} S_{i,j}^{(3)}S_{i,j}^{(1)} \\ \sum_{i,j}^{m} S_{i,j}^{(1)}S_{i,j}^{(2)} & \sum_{i,j}^{m}\left(S_{i,j}^{(2)}\right)^2 & \sum_{i,j}^{m} S_{i,j}^{(3)}S_{i,j}^{(2)} \\ \sum_{i,j}^{m} S_{i,j}^{(1)}S_{i,j}^{(3)} & \sum_{i,j}^{m} S_{i,j}^{(2)}S_{i,j}^{(3)} & \sum_{i,j}^{m}\left(S_{i,j}^{(3)}\right)^2 \end{bmatrix} \begin{bmatrix}\alpha_1 \\ \alpha_2 \\ \alpha_3\end{bmatrix} = \frac{4}{h^2}\begin{bmatrix} \sum_{i,j}^{m}\left(\bar{S}_{i,j} - N\hat{F}_{i,j}\right) S_{i,j}^{(1)} \\ \sum_{i,j}^{m}\left(\bar{S}_{i,j} - N\hat{F}_{i,j}\right) S_{i,j}^{(2)} \\ \sum_{i,j}^{m}\left(\bar{S}_{i,j} - N\hat{F}_{i,j}\right) S_{i,j}^{(3)} \end{bmatrix} \tag{23}$$

ICCS Camera Ready Version 2021
To cite this paper please use the final published version:
DOI: 10.1007/978-3-030-77970-2_19

3.3 Local approximation using independent mesh

In case the unknown source function f is expected to be highly non–linear or localized, the global approximation (17) may provide the general information concerning its values and distribution. On the other hand, monomial terms, which order is higher than 2, may not have a significant influence on the final results. Therefore, a local approximation of f may be assumed, using physical degrees of freedom $\boldsymbol{\alpha} = \mathbf{f}$, based upon a mesh of n_f internal points $\Omega_f = \{\mathbf{x}_f \in \Omega\}$ (Fig 1b). The mesh Ω_f may be totally independent from the approximation mesh $\Omega_h = \{\mathbf{x}_F\}$ for the primary function F, whereas its density may be directly related to the number (m) of measurement locations $\hat{\mathbf{x}}$. Therefore, the additional mapping, between both approximation meshes, namely Ω_f (of function f) and Ω_h (of function F), is required. It may be based upon the Moving Weighted Least Squares (MWLS) approximation technique [18], typical for meshless analysis, in which nodes may be distributed totally arbitrarily, without any imposed structure. Let us assume that the function f is defined by the finite set of its nodal values $\mathbf{f} = f(\mathbf{x}_f)$, given at n_f nodes $\mathbf{x}_f \in \Omega_f$. The function value f as well as its derivatives up to the p–th order are required at the arbitrary point $\mathbf{x}_F \in \Omega_h$. The configuration (called star or stencil) of $m_f < n_f$ nodes $\mathbf{S}_F = \{\mathbf{x}_f\}$, being neighbours of $\mathbf{x}_F$, is assigned to $\mathbf{x}_F$. The meshless star my be generated using various criteria, for instance, a distance criterion in which m_f nodes, closest to $\mathbf{x}$, are selected, or topology oriented ones, like cross or Voronoi neighbours criteria [19]. Afterwards, the local approximation of f is constructed, using the Taylor series expansion, namely

$$f(\mathbf{x}_F, \mathbf{x}) = \mathbf{p}(\mathbf{x}_F - \mathbf{x})\,\mathbf{D}_f(\mathbf{x}_F) \tag{24}$$

where $\mathbf{p}(\mathbf{x}_F - \mathbf{x}) = \left[1 \; |\mathbf{x}_F - \mathbf{x}| \; |\mathbf{x}_F - \mathbf{x}|^2 \; ... \; |\mathbf{x}_F - \mathbf{x}|^p\right]$ is the vector of local interpolants, whereas $\mathbf{D}_f(\mathbf{x}_F) = \left[f \; \frac{\partial f}{\partial x_1} \; \frac{\partial f}{\partial x_2} \; \frac{\partial^2 f}{\partial x_1^2} \; ... \; \frac{\partial^{(p)} f}{\partial x_2^{(p)}}\right]_{\mathbf{x}_F}$ is the vector of subsequent derivatives of f at $\mathbf{x}_F$. Fulfilling of (24) at all m_f node of the $\mathbf{S}_F$ star leads to the over–determined system of linear equations

$$\mathbf{P}(\mathbf{x}_F)\,\mathbf{D}_f(\mathbf{x}_F) = \mathbf{f}(\mathbf{x}_F) \tag{25}$$

where $\mathbf{P}(\mathbf{x}_F) = \mathbf{p}(\mathbf{x}_F - \mathbf{S}_F)$ and $\mathbf{f}(\mathbf{x}_F)$ is the vector of nodal values of f at star nodes. Its solution may be obtained by a minimisation of the weighted error function

$$I(\mathbf{x}_F) = (\mathbf{P}(\mathbf{x}_F)\,\mathbf{D}_f(\mathbf{x}_F) - \mathbf{f}(\mathbf{x}_F))^{\mathrm{T}}\,\mathbf{W}^2(\mathbf{x}_F)\,(\mathbf{P}(\mathbf{x}_F)\,\mathbf{D}_f(\mathbf{x}_F) - \mathbf{f}(\mathbf{x}_F)) \tag{26}$$

Here, $\mathbf{W}(\mathbf{x}_F)$ is the diagonal weighting matrix, with singular weights ω assigned to each node of $\mathbf{S}_F$, according to the formula $\omega(\mathbf{x}_F - \mathbf{x}) = \|\mathbf{x}_F - \mathbf{x}\|^{-p-1}$. Finally, we obtain the matrix of difference formulas

$$\mathbf{M}(\mathbf{x}_F) = \left(\mathbf{P}^{\mathrm{T}}(\mathbf{x}_F)\,\mathbf{W}^2(\mathbf{x}_F)\,\mathbf{P}(\mathbf{x}_F)\right)^{-1}\mathbf{P}^{\mathrm{T}}(\mathbf{x}_F)\,\mathbf{W}^2(\mathbf{x}_F) \tag{27}$$

ICCS Camera Ready Version 2021
To cite this paper please use the final published version:
DOI: 10.1007/978-3-030-77970-2_19

rows of which correspond to difference coefficients of subsequent derivatives in $\mathbf{D}_f$, namely

$$\mathbf{D}_f\left(\mathbf{x}_F\right) = \mathbf{M}\left(\mathbf{x}_F\right)\mathbf{f}\left(\mathbf{x}_F\right) \tag{28}$$

Consequently, the approximation f at nodes $\mathbf{x}_F$ may be substituted into the Monte Carlo relation, yielding the following formula

$$F_{i,j}\left(\mathbf{f}\right) = \frac{1}{N}\left(\sum_{(r,s)\in\partial\Omega_h} \bar{F}_{r,s}\bar{N}_{(i,j),(r,s)} - \frac{h^2}{4}\sum_{(r,s)\in\Omega_h} \mathbf{M}^{\langle 1\rangle}\left(\hat{\mathbf{x}}_{r,s}\right)\mathbf{f}\left(\hat{\mathbf{x}}_{r,s}\right)N_{(i,j),(r,s)}\right) \tag{29}$$

where $\mathbf{M}^{\langle 1\rangle}$ denotes the first row of $\mathbf{M}$. The optimal parameters $\mathbf{f}_{\text{opt}}$ are determined from (20) with (21) and modified terms

$$S_{i,j}^{\{(k),(l)\}} = \sum_{(r,s)\in\Omega_h} M_{1,\{k,l\}}\left(\hat{\mathbf{x}}_{r,s}\right)N_{(i,j),(r,s)} \tag{30}$$

General principles of random walk strategy remain unmodified, namely the selection of four equally probable directions of each next move and its termination at boundary nodes. Moreover, it has to be stressed that for $n_f > m$ the matrix $\mathbf{A}$ from (20) is singular, for $n_f = m$ the matrix $\mathbf{A}$ is ill-conditioned, whereas its conditioning improves as n_f becomes smaller than m. Therefore, appropriate number of measurements m may be required in order to reproduce the source function with assumed accuracy.

4 Numerical examples

Results of selected numerical experiments are presented in order to illustrate the effectiveness of the proposed approach. Since the research is in the preliminary state, only simulated measurement data are taken into account. The following strategy, based upon manufacturing solutions, is adopted

1. Geometry parameters, boundary conditions $\bar{F}$ as well as the right-hand side function f are assumed.
2. The regular mesh $\mathbf{x}_F \in \Omega_h$ is generated and the corresponding direct problem (with known $\bar{F}$ and f) is solved by means of the finite difference method (FDM), yielding the nodal solution $\mathbf{F}$ at $\mathbf{x}_F$.
3. Measurement locations $\hat{\mathbf{x}} \in \Omega_h$ are assumed and measurement data $\hat{\mathbf{F}}$ are generated on the basis of $\mathbf{F}$ values, randomly disturbed with the amplitude ΔF, corresponding to the measurement tolerance.
4. The selected approximation formula ((17) or (24)) for the unknown source function f is assumed, with the optional generation of additional mesh $\mathbf{x}_f \in \Omega_f$ and the mapping $\mathbf{x}_f \to \mathbf{x}_F$.
5. The first inverse solution step: nodal indications are determined at all m measurement locations using standard fixed random walk technique.
6. The second inverse solution step: unknown source parameters $\mathbf{f}$ are determined from the system of equations using appropriate Monte Carlo relations.

ICCS Camera Ready Version 2021
To cite this paper please use the final published version:
DOI: 10.1007/978-3-030-77970-2_19

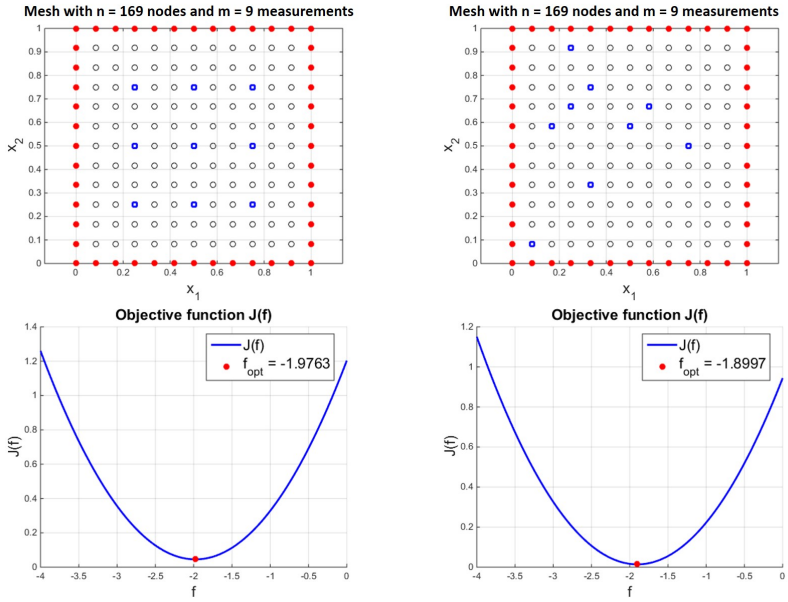

Fig. 2. Objective function and optimal solution for two sets of 9 measurement points

7. The source function f is recovered at all nodes $\mathbf{x}_F \in \Omega_h$ using previously introduced approximation.
8. The resulting direct problem, with recovered function f, is solved by FDM and the primary solution $\mathbf{F}$ is determined at $\mathbf{x}_F \in \Omega_h$.

Preliminary tests are performed for the problem with the constant source intensity $f = -2$, boundary values $\bar{F}(\mathbf{x}) = x_1^2 + x_2^2$, square domain $\Omega = \left[0\ 1\right]^2$, nodes number $n = 13 \times 13$, the number of random walks $N = 1000$, measurements number $m = 3 \times 3$, as well as measurement tolerance $\Delta F = 0.2$ (up to the 10% of the original value). A–priori estimators allow to estimate the approximation error $e_{hp} = Ch^{p+1-k} < 0.0833C$ (with respect to the unknown exact solution), where C is the arbitrary constant, though independent from p and h, as well as the stochastic error (13), namely $e < 0.0316$ (with the respect to the FD solution). Fig. 2 presents results (graph of the objective function and the optimal solution), obtained for fixed parameters, for two types of measurement locations, namely regular and randomly selected distributions. However, the final results of stochastic methods cannot be representative unless they are obtained after appropriate averaging of intermediate results. Therefore, histograms for 1000 various simulations of both random measurement locations and distributions of indication numbers are shown in Fig. 3. It may be observed that the dispersion of results is significant, especially for randomized locations. As a consequence, all following examples are executed in N–based series and properly averaged. Moreover, the influence of selected input parameters on f_{opt} is examined, using

ICCS Camera Ready Version 2021
To cite this paper please use the final published version:
DOI: 10.1007/978-3-030-77970-2_19

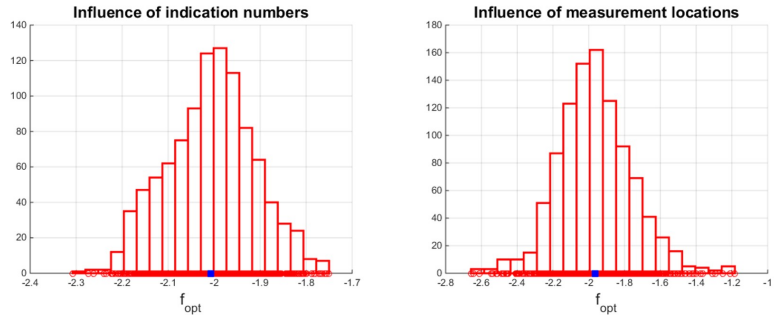

Fig. 3. Histograms of the optimal solution f_{opt}, for variability of indication numbers (left graph) and measurement locations (right graph), for 1000 simulations per 20 classes

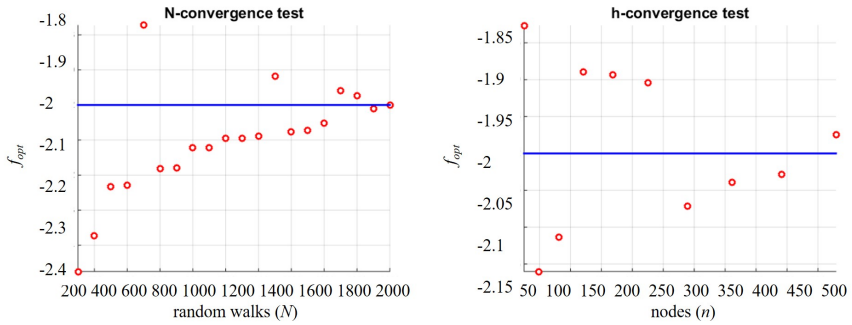

Fig. 4. Results of N-convergence (left graph) and h-convergence tests (right graph)

the regular grid of $m = 9$ measurement points. Fig. 4 presents convergence of f_{opt} with respect to N (with fixed h, m and ΔF) and h (with fixed N, m and ΔF), whereas Fig. 5 shows convergence of f_{opt} with respect to m (with fixed N, h and ΔF) and Δ (with fixed N, h and m). Each time, results are stable and convergent to the original intensity value ($f = -2$). Afterwards, the global monomial approximation (17) of the full second order ($n_f = 6$) is applied for the recovery of the unknown source function. The simulated measurement data ($m = 9$, $\Delta F = 10\%$ of the original value) are generated on the basis of the FDM solution, obtained on the regular mesh with $n_F = 81$ nodes and corresponding to the original source function $f(\mathbf{x}) = -2 + x_1 + 3x_2 - 5x_1^2 + x_1x_2 + 7x_2^2$. Nodal indications are determined by means of 10 series of $N = 1000$ random walks. Results are presented in Fig. 6. The formula of the recovered source function as well as relative source and solution errors, evaluated in L^2 and max norms, are given in graphs' titles. The maximum errors are approx. 2% (for f) and 1% for (F). Eventually, the local approximation of the first order as well as the independent mesh for the approximation of f are applied for the recovery of the source function, given by more complex formula of exponential type, namely

ICCS Camera Ready Version 2021
To cite this paper please use the final published version:
DOI: 10.1007/978-3-030-77970-2_19

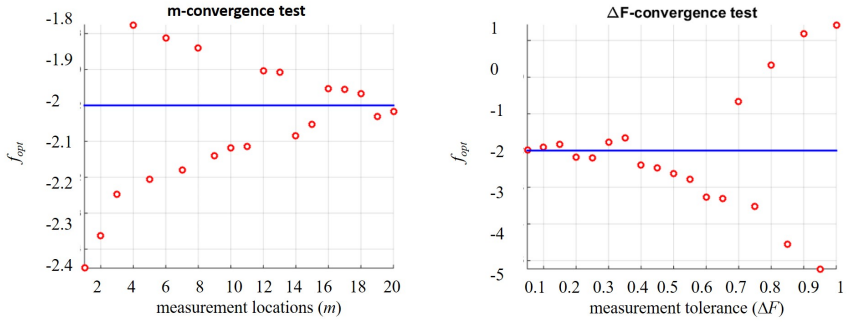

Fig. 5. Results of m-convergence (left graph) and ΔF-convergence tests (right graph)

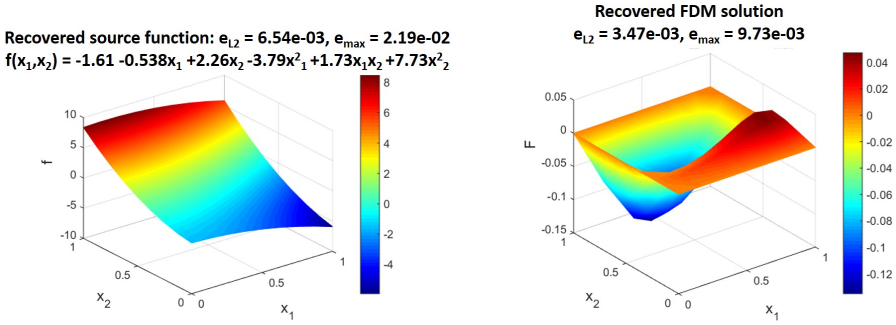

Fig. 6. Recovered source function f (left graph) and primary solution F (right graph) using global approximation and mathematical degrees of freedom

$f(\mathbf{x}) = \exp\left(-5\left(x_1^2 + (x_2 - 9/10x_1)^2\right)\right)$. It may be computationally demanding even for the direct problem as it requires a dense discretization mesh and, therefore, a vast computational power. The applied model is based upon the approximation mesh with $n_F = 225$ nodes and $m = 49$ measurements, as well as the regular grid for the source function approximation with $n_f = 36$ physical degrees of freedom $\mathbf{f}$. Results are presented in Fig. 7. Relative source and solution errors, evaluated in L^2 and max norms, are given in graphs' titles. Similarly as in the previous example, the maximum errors are reasonably small, namely approx. 2.5% (for f) and 1% for (F). Furthermore, in all cases, the computational times are negligible (below several seconds). All results are obtained on 16 GB RAM and 1.80 GHz processor, using author's original software, written in Matlab R2014b.

5 Final remarks

The semi–analytical approach for the numerical analysis of inverse Poisson problems is presented. In inverse Poisson problem, the source (load) function is un-

ICCS Camera Ready Version 2021
To cite this paper please use the final published version:
DOI: 10.1007/978-3-030-77970-2_19

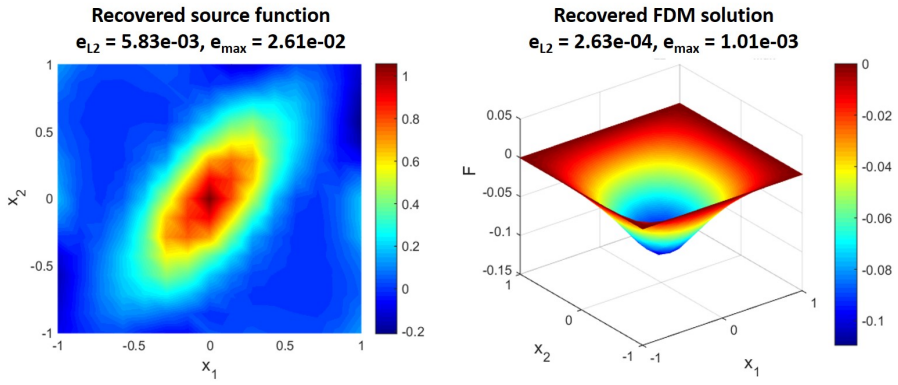

Fig. 7. Recovered source function f (left graph) and primary solution F (right graph) using local approximation and physical degrees of freedom

known, whereas set of measurements of the primary function, being the solution to this problem, may constitute the additional data. The problem may be formulated as the non–linear optimisation problem, in which the objective function is the average error between the measured and computed values whereas decision variables are source function parameters. The proposed approach is based upon the old and well–known concept of the Monte Carlo method as well as random simulations (random walks), performed on the regular mesh of points. It incorporates several features of the standard (selection probabilities) and meshless (mapping between independent meshes) finite difference methods. On the contrary to the standard optimisation methods, this approach requires neither an iterative procedure nor a searching of the admissible solution space. The optimal source functions parameters are determined from the system of linear equations, which source is the analytical differentiation of the objective function, approximated in the coupled stochastic-deterministic manner.

The future work may include the generalisation of the proposed approach for more complex geometries, for which unstructured meshes and arbitrarily irregular clouds of nodes are required as well as for problems with mixed boundary conditions. Selection directions and probabilities may be determined using meshless approximation techniques, similar to those already applied in the mapping between two independent approximation meshes. Moreover, the application of the approach to inverse problems of non–stationary thermal as well as to linear elastic types is planned.

References

1. Jiang, J., Mohamed, SM., Seaid, M., Li, H.: Identifying the wavenumber for the inverse Helmholtz problem using an enriched finite element formulation, Computer Methods in Applied Mechanics and Engineering **340**, 615–629 (2018)

ICCS Camera Ready Version 2021
To cite this paper please use the final published version:
DOI: 10.1007/978-3-030-77970-2_19

2. Ohe, T., Ohnaka, K.: Boundary element approach for an inverse source problem of the Poisson equation with a one-point-mass like source. Applied Mathematical Modelling **18**(4), 216–223 (1994)
3. Gu, Y., Lei, J., Fan, CM., He, XQ.: The generalized finite difference method for an inverse time-dependent source problem associated with three-dimensional heat equation. Engineering Analysis with Boundary Elements **91**, 73–81 (2018)
4. Khan, MN., Ahmad, I., Ahmad, H.: A radial basis function collocation method for space-dependent inverse heat problems. Journal of Applied and Computational Mechanics DOI: 10.22055/jacm.2020.32999.2123 (2020)
5. Hamad, A., Tadi, M.: A numerical method for inverse source problems for Poisson and Helmholtz equations. Physics Letters A **380**(44), 3707–3716 (2016)
6. Koulouri, A., Rimpiläinen, V., Brookes, M., Kaipio, JP.: Compensation of domain modelling errors in the inverse source problem of the Poisson equation: Application in electroencephalographic imaging. Applied Numerical Mathematics **106**, 24–36 (2016)
7. Rond, A., Giryes, R., Elad, M.: Poisson inverse problems by the Plug-and-Play scheme. Journal of Visual Communication and Image Representation **41**, 96–108 (2016)
8. Alves, C., Martins, N., Roberty, N.: Full identification of acoustic sources with multiple frequencies and boundary measurements. Inverse Problems and Imaging **3**(2), 275–294 (2009)
9. Frackowiak, A., Wolfersdorf, JV., Ciałkowski, M.: Solution of the inverse heat conduction problem described by the Poisson equation for a cooled gas-turbine blade. International Journal of Heat and Mass Transfer **54**(5–6), 1236–1243 (2011)
10. Bergagio, M., Li, H., Anglart, H.: An iterative finite-element algorithm for solving two-dimensional nonlinear inverse heat conduction problems. International Journal of Heat and Mass Transfer **126**(A), 281–292 (2018)
11. Wen, H., Yan, G., Zhang, C., He, X.: The generalized finite difference method for an inverse boundary value problem in three-dimensional thermo-elasticity. Advances in Engineering Software **131**, 1–11 (2019)
12. Wang, X., Li, H., He, L., Li, Z.: Evaluation of multi-objective inverse heat conduction problem based on particle swarm optimization algorithm, normal distribution and finite element method. International Journal of Heat and Mass Transfer **127**(A), 1114–1127 (2018)
13. Milewski S.: Determination of the truss static state by means of the combined FE/GA approach, on the basis of strain and displacement measurements. Inverse Problems in Science and Engineering, **27**(11), 1537–1558 (2019)
14. Liu, JC., Li, XC.: Reconstruction algorithms of an inverse source problem for the Helmholtz equation. Numerical Algorithms **84**, 909–933 (2020)
15. Reynolds, JF.: A Proof of the Random-Walk Method for Solving Laplace's Equation in 2-D. The Mathematical Gazette **49**(370), 416–420 (1965)
16. Milewski S.: Combination of the meshless finite difference approach with the Monte Carlo random walk technique for solution of elliptic problems. Computers & Mathematics with Applications, **76**(4), 854–876 (2018)
17. Milewski S.: Application of the Monte Carlo method with meshless random walk procedure to selected scalar elliptic problems. Archives of Mechanics, **71**(4-5), 337–375 (2019)
18. Lancaster, P., Salkauskas, K.: Curve and surface fitting. An introduction, Academic Press Inc, London, 1st edition:280 pages (1990)
19. Orkisz, J.: Handbook of computational solid mechanics: Finite difference method (Part III), Springer-Verlag, Berlin, 1st edition:336–431 (1998)

ICCS Camera Ready Version 2021
To cite this paper please use the final published version:
DOI: 10.1007/978-3-030-77970-2_19